Supplemental: Spatial heterogeneities in structural temperature cause Kovacs' expansion gap paradox in aging of glasses

Matteo Lulli,[1,2] Chun-Shing Lee,[1] Hai-Yao Deng,[3,4] Cho-Tung Yip,[5] and Chi-Hang Lam[1,*]

[1] *Department of Applied Physics, Hong Kong Polytechnic University, Hong Kong, China*
[2] *Department of Mechanics and Aerospace Engineering, Southern University of Science and Technology, Shenzhen, Guangdong 518055, China*
[3] *School of Physics, University of Exeter, Exeter EX4 4QL, United Kingdom*
[4] *School of Physics and Astronomy, Cardiff University, The Parade, Cardiff CF24 3AA, United Kingdom*
[5] *School of Science, Harbin Institute of Technology, Shenzhen Graduate School, Shenzhen, Guangdong 518055, China*

(Dated: January 27, 2020)

I. DPLM DEFINITION AND SIMULATIONS

In the simulations we have performed, the DPLM is defined on a 2-dimensional square lattice of linear size $L = 100$. The sites are occupied by N distinguishable particles, each of them associated to a *unique label* ranging from 1 to N. Then, $s_i = 1, \ldots, N$ denotes the label of the particle at site i. The key feature of the model is that each particle is coupled to its nearest neighbors by means of *site-* and *particle-dependent* random interactions: a four-indices interaction energy $V_{ijs_is_j}$ is associated to the particles s_i and s_j sitting at sites i and j. In order to simulate the hopping dynamics of the particles we allow for the presence of empty sites or *voids*. Considering a void density $\phi_v = N_v/L^2 = 0.005$, in a system of linear size $L = 100$ there are $N_v = 50$ voids with default label $s_i = 0$, hence $L^2 = N + N_v$.

The interactions are symmetric under concurrent exchange of spatial and particle indices, i.e. $V_{ijkl} = V_{jilk}$. The entire set of possible interactions $\{V_{ijkl}\}$ is drawn according to an *a priori* probability distribution $g(V)$ and it is *quenched*. For each equilibrium particle configuration, there is a set $\{V_{ijs_is_j}\}$ of interactions which are referred to as *realized* and it has been shown that they are distributed according to p_{eq} [1]

$$p_{eq}(V,T) = \frac{1}{\mathcal{N}(T)}\, g(V)\, e^{-V/k_BT}, \tag{1}$$

where $\mathcal{N}(T)$ is a temperature-dependent normalization.

The kinetic Monte Carlo simulations implement an activated-hopping dynamics for which each particle can hop to the position of a neighboring void with a rate

$$w = w_0 \exp\left[-\frac{1}{k_BT}\left(E_0 + \frac{\Delta E}{2}\right)\right], \tag{2}$$

where ΔE is the energy change of the system induced by the hop. We set $w_0 = 10^6$ and $E_0 = 1.5$ so that $E_0 + \Delta E/2 \geq 0$.

The data reported in Fig. 1 of the main text are obtained from $2^{17} \simeq 1.3 \times 10^5$ independent runs with different random number seeds and the jackknife resampling method is used for computing averages and errors of $\tau_{\rm eff}$.

Finally, we notice that $\tau_{\rm eff}^{-1}$ in Fig. 1(b) of the main text does not exhibit a gentle rise at intermediate values of δ_E for the up-jumps as observed in experiments [2]. This may happen because we have adopted, for simplicity, a constant void density ϕ_v in our simulations, which should instead increase upon heating. Such an increase of ϕ_v would yield a faster dynamics

II. THERMAL PROPERTIES OF THE DPLM

In the main text, we discuss about the final equilibrium value of the system energy E_∞ and the specific heat as a function of the temperature. Let us now derive in detail these two quantities. In order to obtain the equilibrium energy E_∞ as a function of the temperature T one has to compute the average of the system energy [see Eq.(1) in the main text]

$$E_\infty(T) = \sum_{\langle ij\rangle'} \langle V_{ijs_is_j}\rangle_T = N_b \int_{V_0}^{V_1} \mathrm{d}V\, V\, p_{eq}(V,T), \tag{3}$$

where $[V_0, V_1]$ is the range of variation of the couplings, N_b is the average number of bonds and p_{eq} is the equilibrium distribution of the interaction energies given in Eq. (1). A good estimate of N_b, at a low void density, can be obtained in the approximation of isolated voids, i.e. a void does not have another void as a nearest neighbor, yielding in two dimensions $N_b = 2L^2 - 4N_v \simeq 2N(1-\phi_v)$, where $2L^2$ is the number of interactions for the fully occupied lattice while each isolated void decreases this number by the 4 missing couplings with its nearest neighboring particles. Hence, the problem reduces to computing the average interaction energy as a function of the temperature, i.e. $\langle V\rangle_T$. In this paper we choose $g(V)$ as a uniform distribution, i.e. $g(V) = 1/\Delta V$ where $\Delta V = V_1 - V_0$ is the range of variation of the interactions.

* C.H.Lam@polyu.edu.hk

The general expression reads

$$E_\infty(T) = 2N(1-\phi_v)\left[V_0 + k_BT - \Delta V \frac{e^{-\Delta V/k_BT}}{1-e^{-\Delta V/k_BT}}\right], \tag{4}$$

which, choosing the boundary values as $V_1 = -V_0 = 1/2$, reduces to

$$E_\infty(T) = 2N(1-\phi_v)\left[k_BT - \frac{1}{2}\coth\left(\frac{1}{2k_BT}\right)\right]. \tag{5}$$

It is easy to check that, in this case, $E_\infty(T) \leq 0$ where the equality holds in the limit $T \to \infty$. By taking the derivative with respect to the temperature, we write the heat capacity in the general case as

$$C_V(T) = 2k_BN(1-\phi_v)\left\{1 - \left(\frac{\Delta V}{2k_BT}\right)^2 \sinh^{-2}\left(\frac{\Delta V}{2k_BT}\right)\right\}. \tag{6}$$

One can verify that $\mathrm{d}C_V(T)/\mathrm{d}T < 0$, hence C_V is a decreasing function of T as highlighted in the main text.

III. DYNAMIC STABILITY

The structural temperature heterogeneity, appearing during the up-jump, can be understood in terms of a stability argument of propagating fronts. First, the heating up of a glass is an auto-catalytic process, since the excitation of particle arrangements to higher-energy configurations speeds up the particle dynamics and hence provides a positive feedback to the further warming of the system. In d dimensions, $T_S(\vec{x},t)$ can be seen as a succession of equal-time d-dimensional surfaces in a $(d+1)$-dimensional space, representing a front propagating upwards from T_i to T_f. The propagation is driven by the energy influx from the bath and is stochastic because of the intrinsic noise of the particles dynamics. The evolution of the surfaces is unstable against small perturbations, meaning that a locally out-stretched (warmer) region will further advance much faster towards the final value T_f as the auto-catalytic nature of the dynamics amplifies the perturbations. For very low T_i, implying an extreme sensitivity of the dynamics on temperature, T_S can comparatively quickly reach T_f in localized domains, while being practically stuck at the initial value T_i elsewhere. This explains the nucleation of T_f domains in a background of T_i regions. The fast dynamics in T_f domains enhances the heating-up of neighboring regions, inducing domain-wall motions. Due to the very stable configurations of the T_i regions, the domain invasion can be a slow process compared with the relaxation dynamics in the T_f domains. Therefore, the particle displacement $d(\vec{x},t)$ can become very large in the mobile T_f domains even close to their domain boundaries as observable in Fig. 2 of the main text. By contrast, cooling for the down-jump protocol is instead an auto-retarding process so that the downward propagating front $T_S(\vec{x},t)$ is stable against perturbations. The dynamics is thus overall homogeneous with relatively uniform $T_S(\vec{x},t)$ as shown in Fig. 2 of the main text.

IV. OBSERVABLES AND DOMAINS DETECTION

We define a *local particle displacement* $d(\vec{x},t) = |\vec{x}-\vec{x}_0|$ as the distance of a particle located at $\vec{x}$ at time t relative to its position $\vec{x}_0$ at time 0 when the temperature jump is imposed. If $\vec{x}$ is vacant at time t, we put $d(\vec{x},t) = 0$ for simplicity. It is useful to define a local particle persistence, i.e. an *overlap* field, $\tilde{q}(\vec{x},t)$ as

$$\tilde{q}(\vec{x},t) = \begin{cases} 1 & \text{if} \quad d(\vec{x},t) = 0 \\ 0 & \text{if} \quad d(\vec{x},t) > 0 \end{cases} \tag{7}$$

such that the average overlap $q(t)$, i.e. $\tilde{q}(\vec{x},t)$ averaged over sites occupied at t, gives the fraction of particles still located at their original positions at time t.

In order to characterize the up-jump scenario of nucleation and coarsening dynamics of the high-T_S mobile domains (see Fig. 2 of the main text) we resorted to a procedure allowing us to identify each domain and study the time evolution of the average area. To do so we employed the module `scipy.ndimage.measurements.label` of the SciPy [3] Python library using a next-to-nearest neighbors stencil and adapting the output to handle periodic boundary conditions. Specifically, the complementary overlap field is defined as $\tilde{q}_c(\vec{x},t) = 1-\tilde{q}(\vec{x},t)$ (see Eq.(2) in the main text), so that $\tilde{q}_c(\vec{x},t) = 1$ signifies a mobile site. A mobile domain consists of connected mobile sites, where connections can be along nearest or next-nearest neighboring lattice edges.

A simple, yet very informative, observable that can be readily obtained from this analysis is the number of mobile domains N_d. Its evolution for up- and down-jumps is reported in Fig. 3(e) of the main text. The initial growth of N_d in the up-jump case signals the nucleation of mobile domains.

A further step can be made by looking at the dynamics of the average area

$$\langle A_i(t)\rangle = \frac{1}{N_d(t)} \sum_{i=1}^{N_d(t)} A_i(t) \tag{8}$$

which is reported in the main text in Fig. 3(f).

V. OVERLAP AND VOID DYNAMICS

In the main text, we report the evolution of different quantities, in Fig. 2 and 3, as a function of the average overlap rather than as a function of time. This choice is motivated by the fact that the differences in the dynamics between down- and up-jump are most clearly visible when measuring the evolution in terms of the fraction

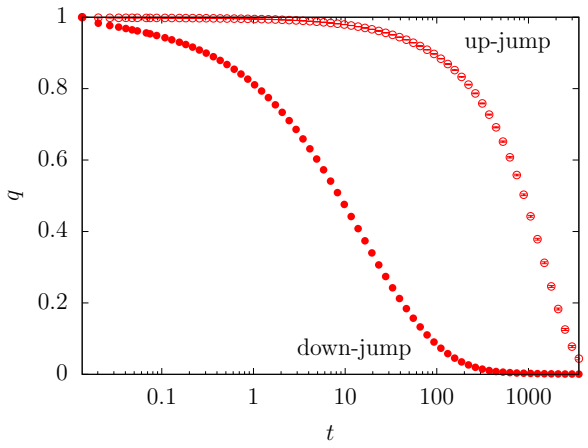

FIG. 1. Average overlap evolution, $q(t)$, for up-jump with $T_i = 0.1$ and down-jump with $T_i = 0.3125$, with a common final temperature $T_f = 0.25$. These values are the same as those used in Fig. 2 of the main text.

of particles that still retain the position $\vec{x}_0$ at the moment when the temperature jump is performed, i.e. the average overlap q as discussed in the main text. Hence, we report in Fig. 1 the evolution of the average overlap as a function of time, where the much slower up-jump relaxation is clearly visible.

Finally, we report here in Fig. 2 the positions of the voids for three of the configurations shown in Fig. 2 of the main text. We notice that for the down-jump dynamics all the voids belong to the mobile region already at an early stage, while for the up-jump some voids stay *trapped* in the immobile regions. The void and field dynamics can be examined also from the supplementary videos *supvideo_up.mp4* and *supvideo_down.mp4*.

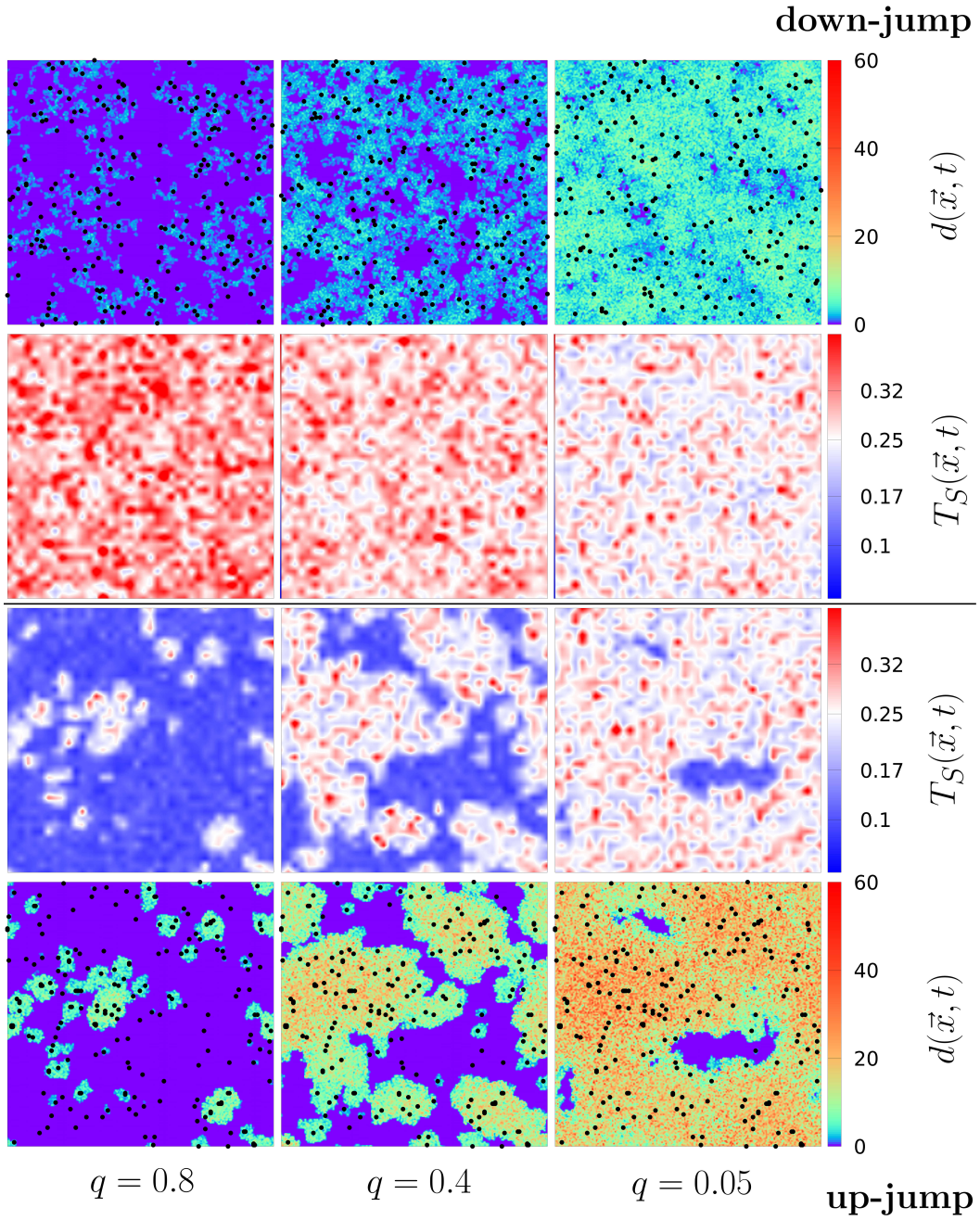

FIG. 2. Three of the four snapshots reported in Fig.1 of the main text with the void positions reported by black dots. The initial temperatures are $T_i = 0.3125$ and $T_i = 0.1$ for the down- and up-jump respectively, with the final temperature $T_f = 0.25$.

[1] L.-H. Zhang and C.-H. Lam, Phys. Rev. B **95**, 184202 (2017).
[2] A. J. Kovacs, in *Fortschritte Der Hochpolymeren-Forschung* (Springer Berlin Heidelberg, Berlin, Heidelberg, 1964) pp. 394–507.
[3] E. Jones, T. Oliphant, P. Peterson, *et al.*, "SciPy: Open source scientific tools for Python," (2001–).